

Supplementary Materials for  
**Spatial resolution of an integrated C<sub>4</sub>+CAM photosynthetic metabolism**

Jose J. Moreno-Villena *et al.*

Corresponding author: Jose J. Moreno-Villena, josejmovi@gmail.com; Haoran Zhou, haoran.zhou@yale.edu

*Sci. Adv.* **8**, eabn2349 (2022)  
DOI: 10.1126/sciadv.abn2349

**The PDF file includes:**

Figs. S1 to S8  
Tables S1 to S8  
Legends for tables S1 to S5

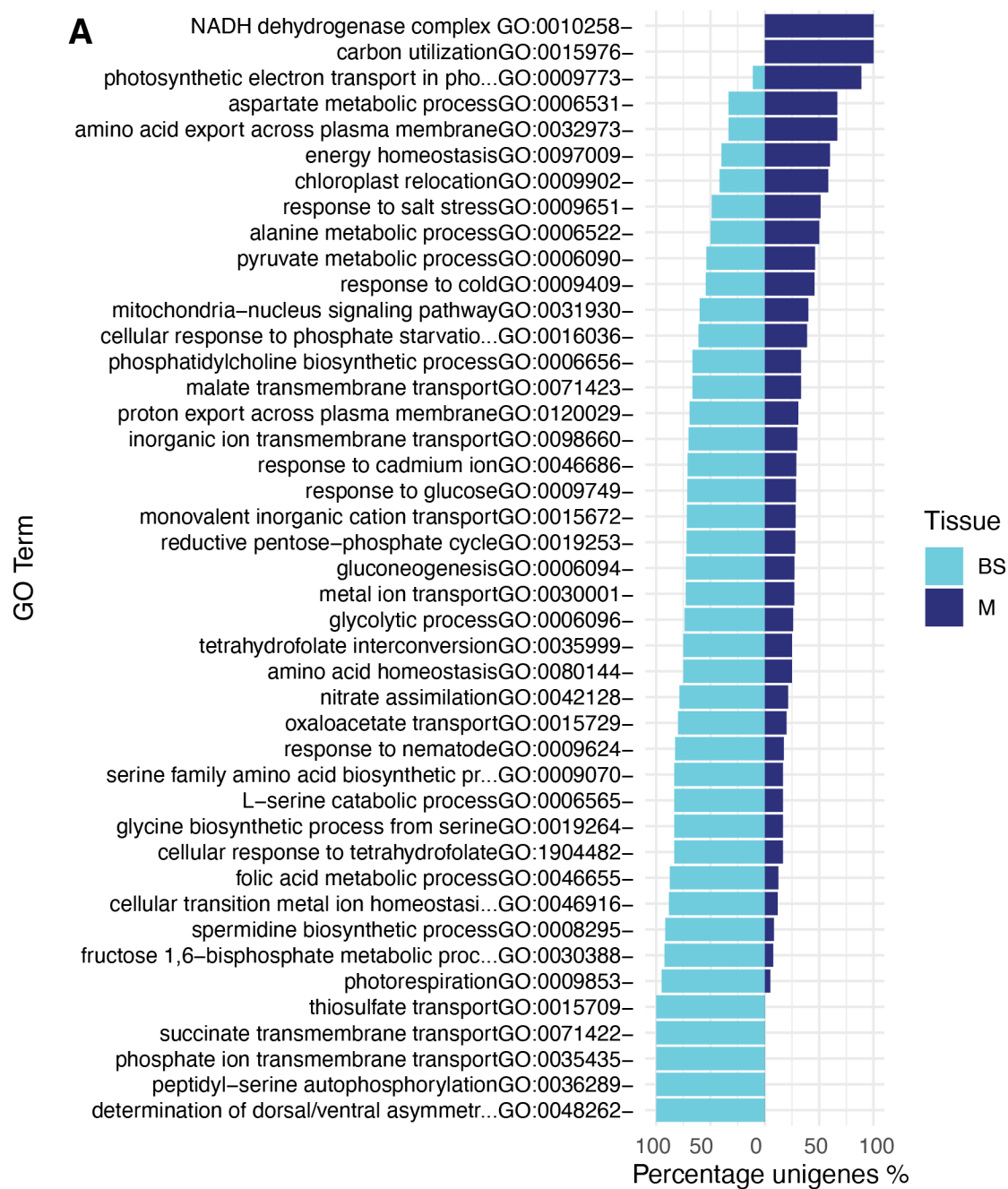
**Other Supplementary Material for this manuscript includes the following:**

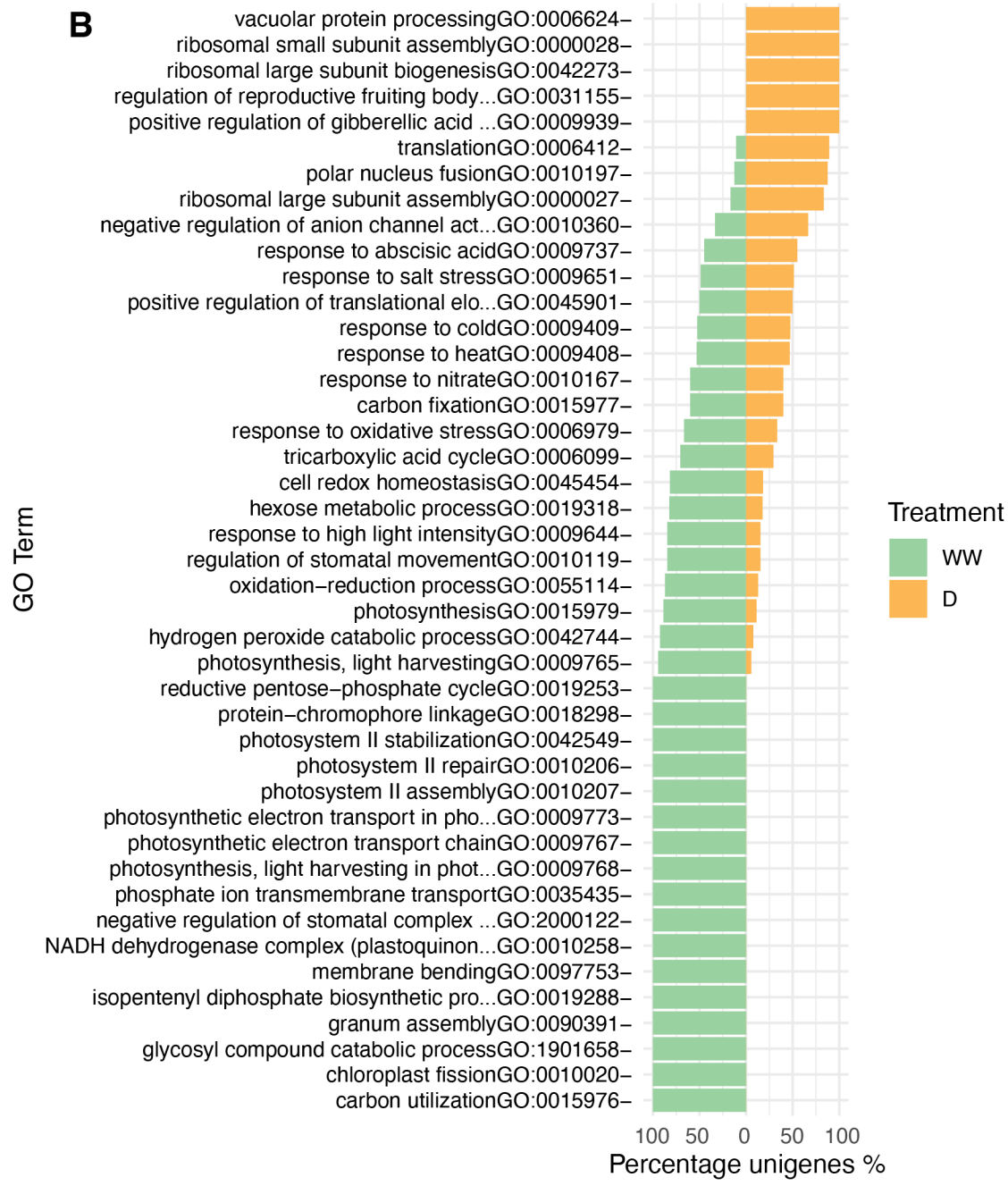
Tables S1 to S5  
Data files S1 to S6

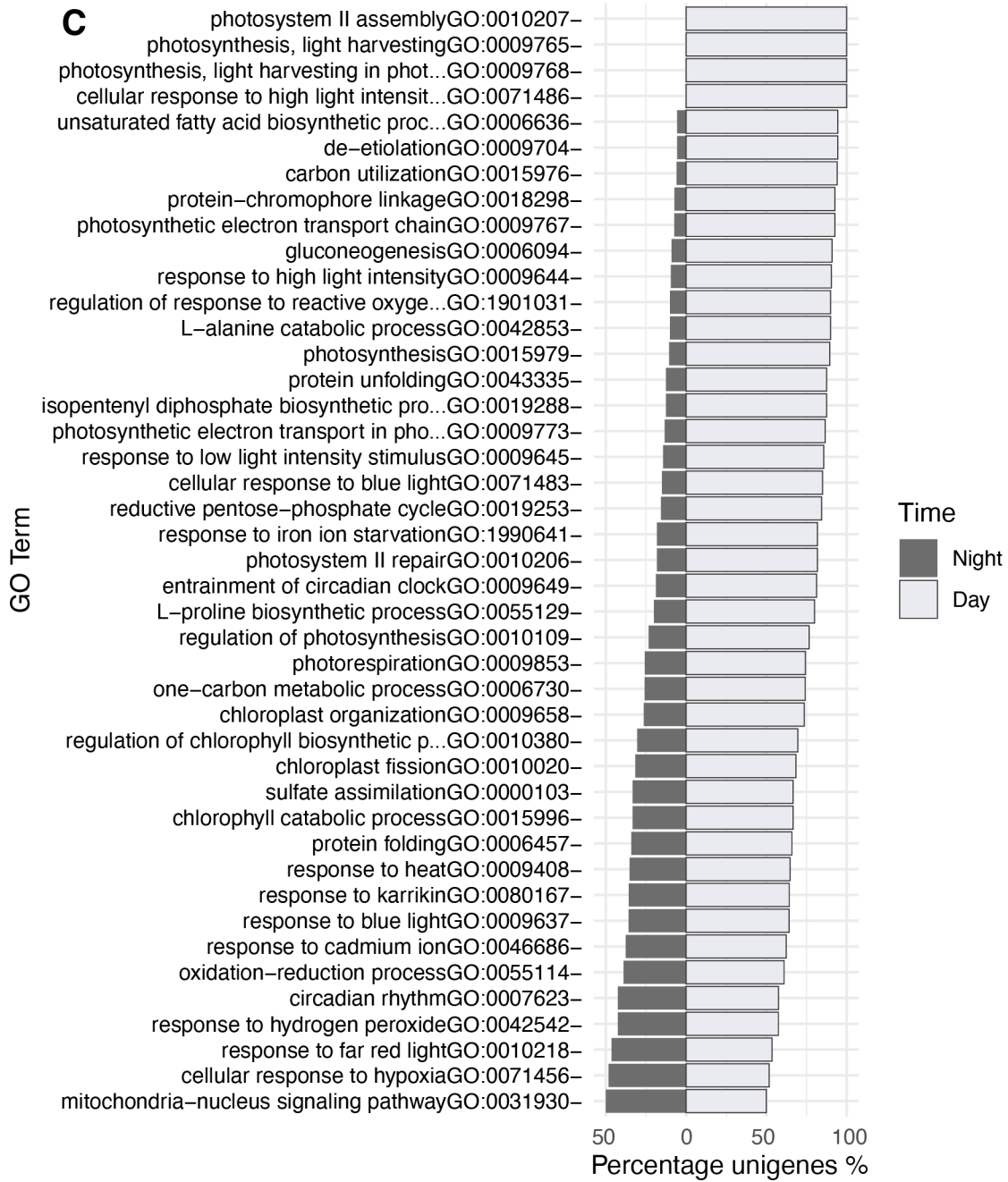
## Supplementary figures

Fig. S1.

**Gene Ontology enrichment across bundle sheath and mesophyll and across watering regimens.** 50 most significant Gene Ontology terms enriched across differentially expressed genes between mesophyll and bundle sheath. Barplots indicate the percentage of genes up-regulated of each GO term across (A) mesophyll and bundle sheath, (B) well-watered and drought, (C) 23h and 7h.







**Fig. S2.**

**Differential transcript abundance across cell types and experimental conditions.**

**(Extension fig. 3)** Differential transcript abundance (measured in log2 fold change, log2FC) of selected genes in mesophyll (M) relative to bundle sheath (BS) tissue (left panel), 07h relative to 23h (middle panel) and drought relative to well-watered (right panel) across LMD samples. Gene colour backgrounds correspond with pathways in the boxes on the top. In all panels, asterisks indicate significant differential expression ( $P_{adj} < 0.05$ ).

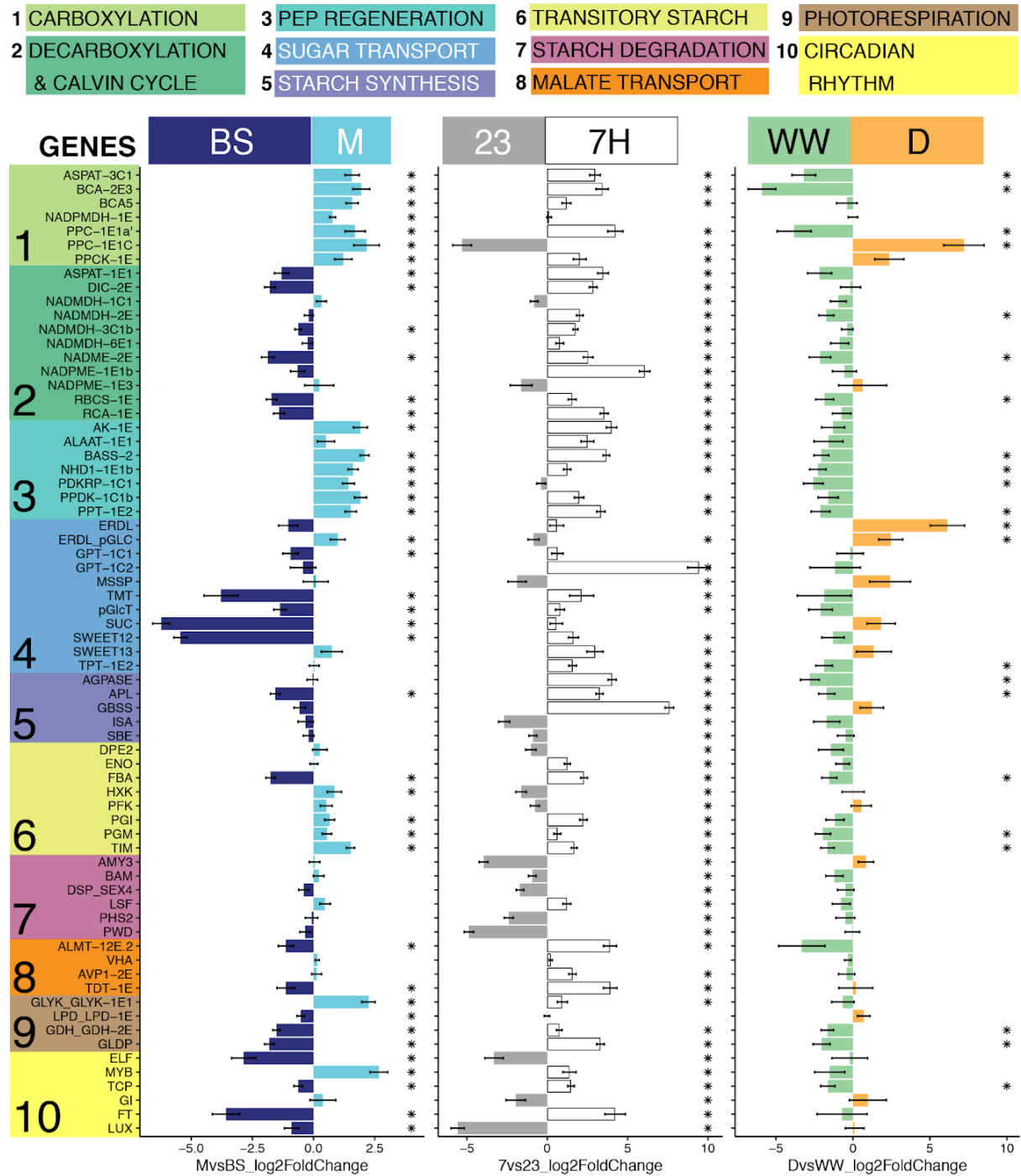


**Fig. S3.**

**Effect of watering regimen in each cell type across time points (extension fig. 3).**

Differential transcript abundance in droughted:D relative to well-watered plants:WW (measured in log<sub>2</sub> fold change, log<sub>2</sub>FC). Gene colour backgrounds correspond to pathways in the boxes on the top. Triangles on the left panel represent relative abundance of D mesophyll samples vs WW mesophyll, in 7h samples (white triangles) and in 23h samples (black triangles). Right panel shows the same abundance comparisons using only bundle sheath samples. A triangle in the WW region (negative log<sub>2</sub>FC, left to the red lines) indicates higher expression during WW, while triangles within the D region (right to the red line) indicate higher expression in D. Asterisks indicate significant differential expression (*P*<sub>adj</sub> < 0.05)

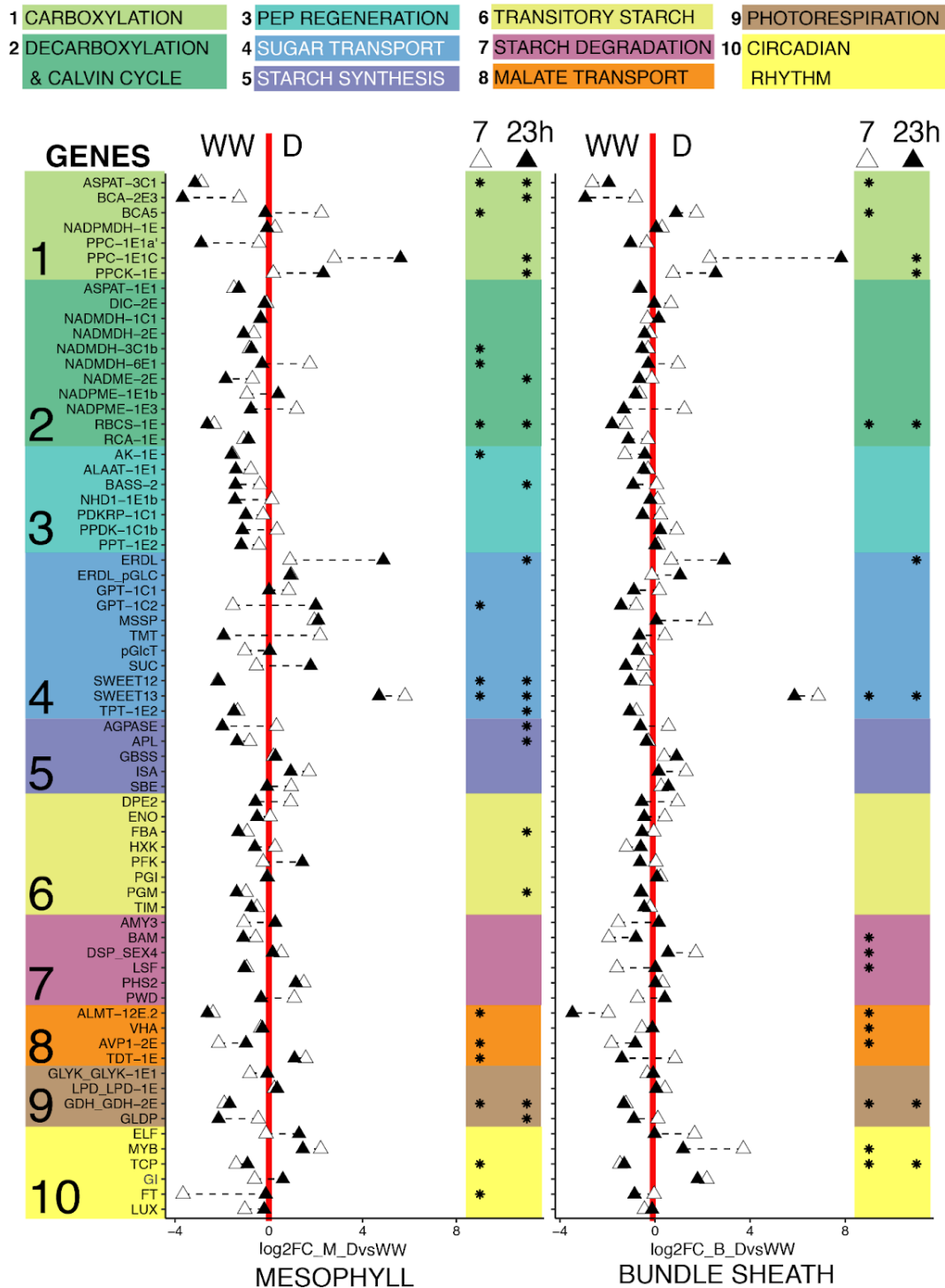
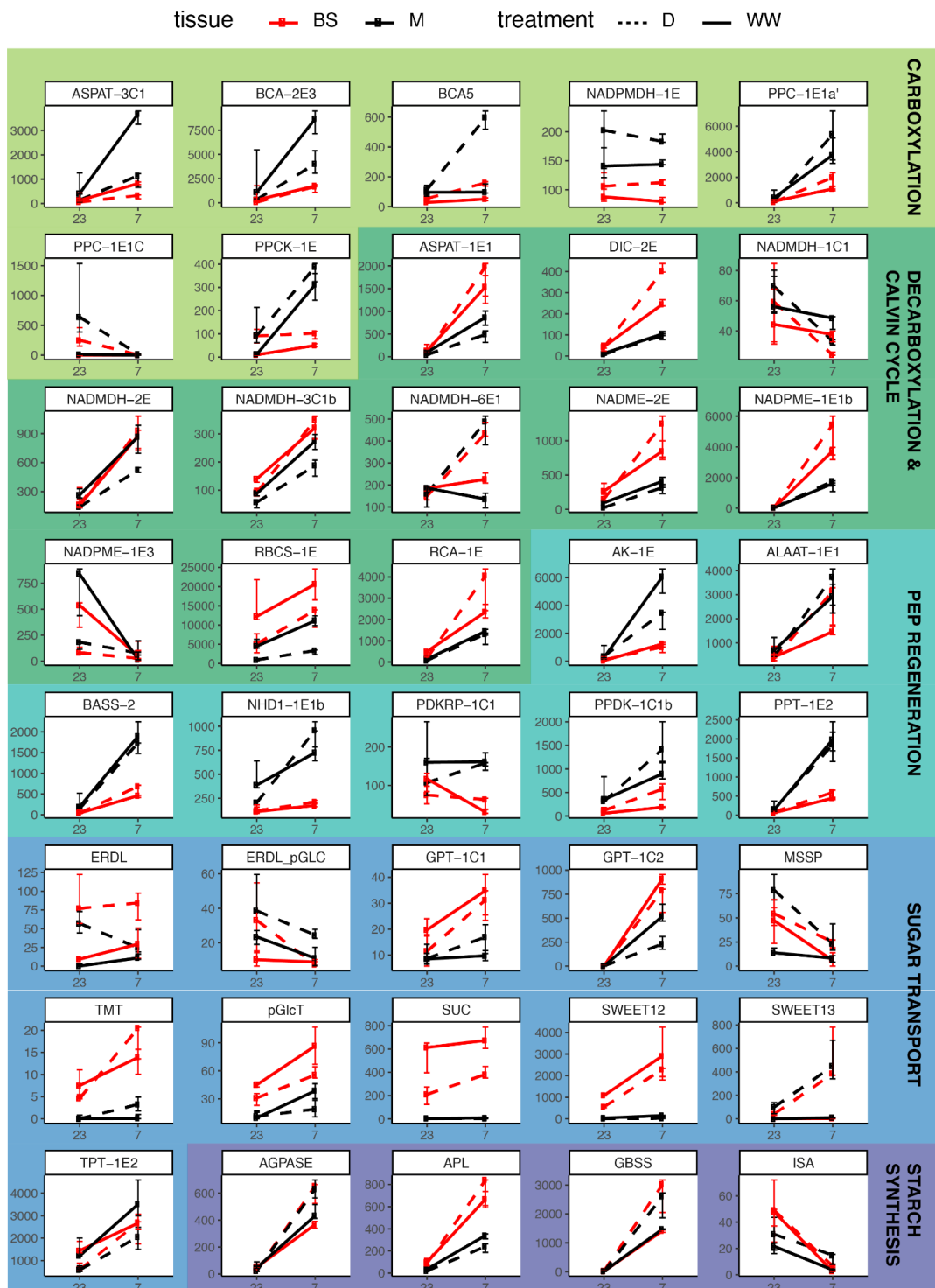


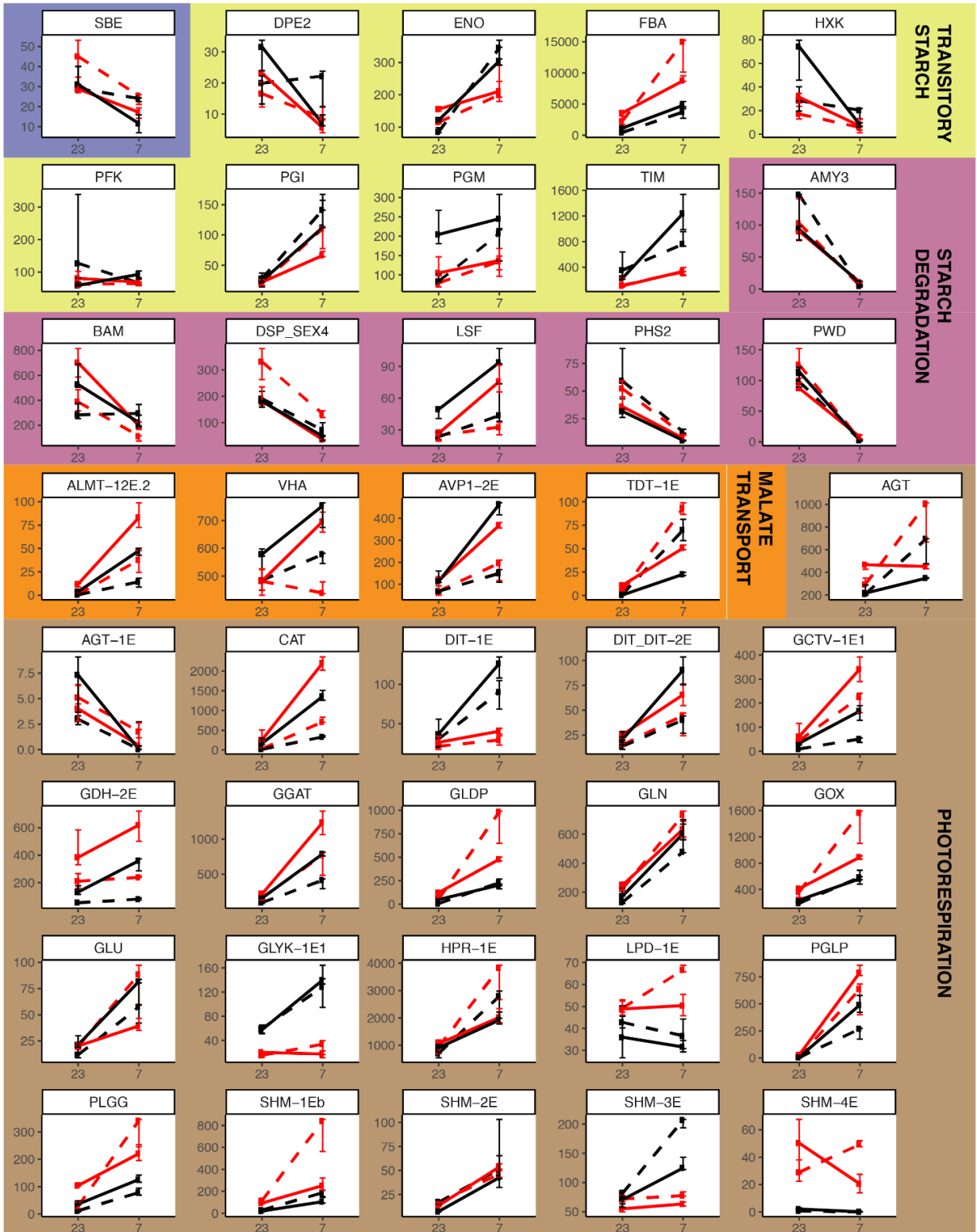
**Fig. S4.**

**Transcription abundance of CCM-related genes.** Transcription abundance of genes listed in table S3 as the median of transcripts per million (y-axis), across time points (x-axis) in LMD mRNA libraries. Black and red lines indicate mesophyll or bundle sheath, respectively. Plain lines indicate watered and dotted indicate drought. Error bars show interquartile range of expression.





tissue ■ BS ■ M treatment - - - D — WW





tissue —■ BS —■ M treatment - - - D — WW

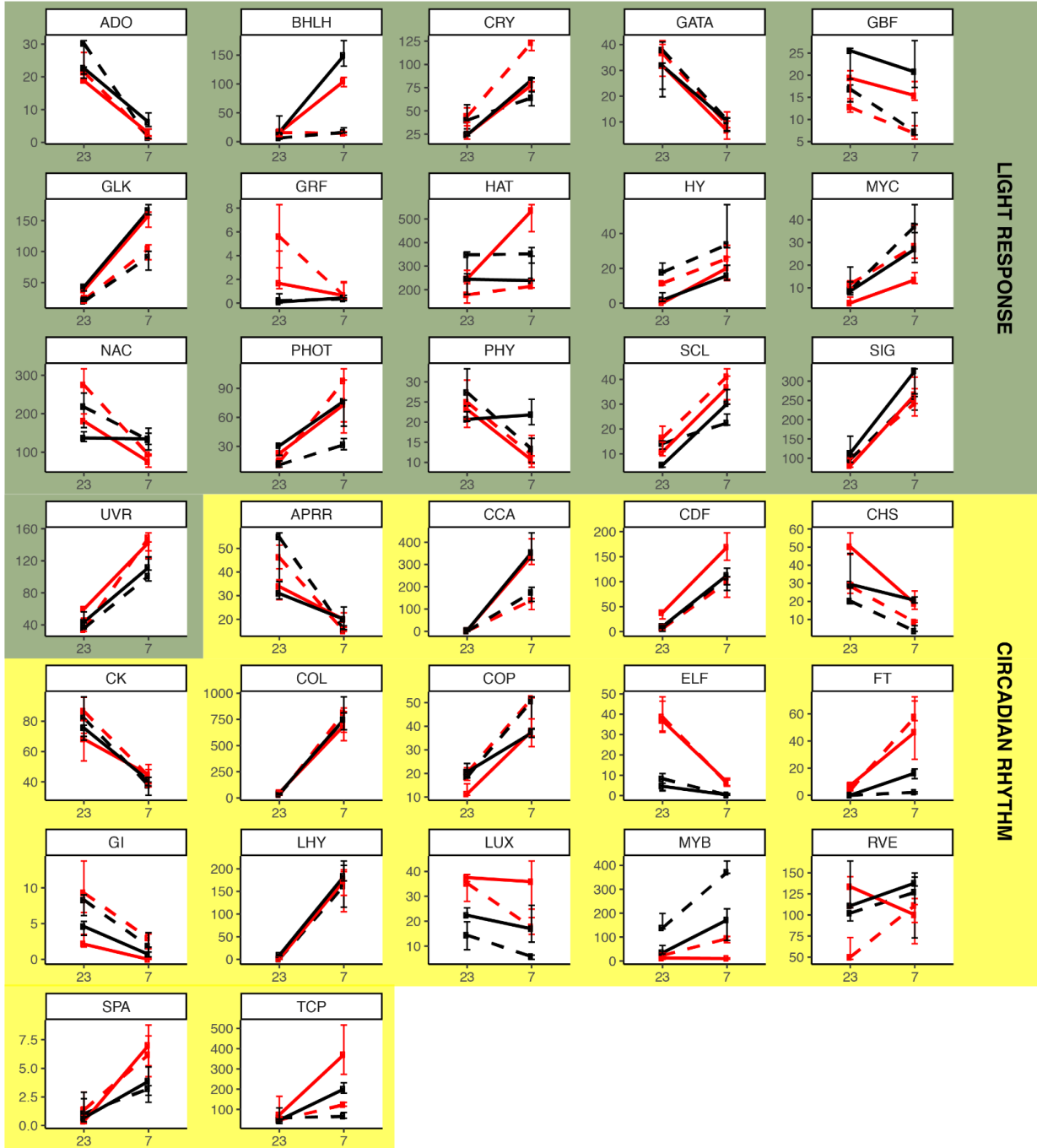


**Fig. S5.**

**Transcription abundance of genes with no known role in C4 or CAM.** (Genes listed in table S4) Median of transcripts per million (y-axis), across time points (x-axis) in LMD mRNA libraries. Black and red lines indicate mesophyll or bundle sheath, respectively. Plain lines indicate watered and dotted indicate drought. Error bars show the interquartile range of expression.

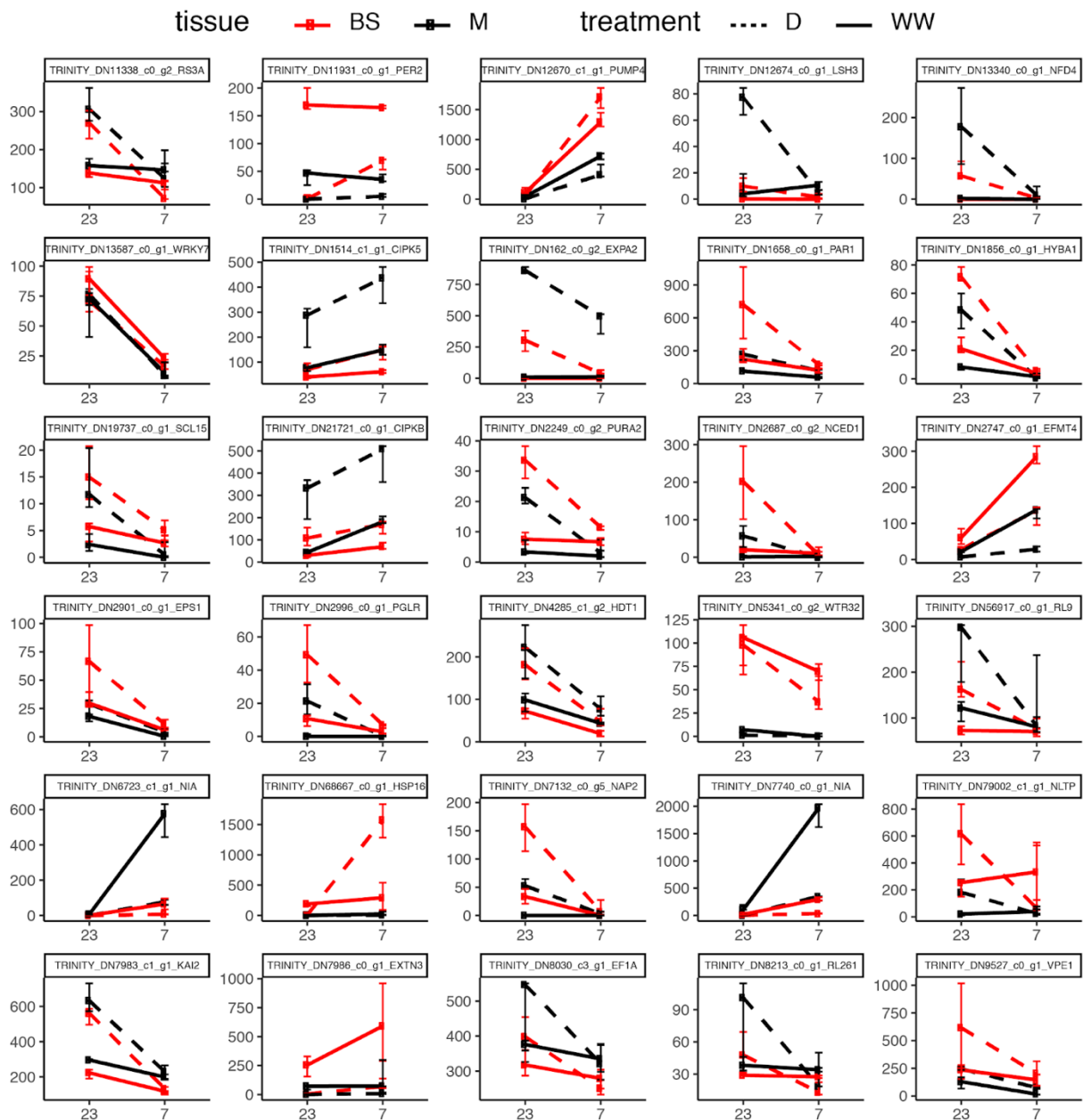


**Fig. S6.**

**Visium spatial gene expression.** The first row shows frozen leaf specimens at the moment of cryo-sectioning. The second row shows microphotographs of leaf paradermal sections under bright field (left) and K-means clustering of total gene expression (right). Successive rows show abundance of the main CCM-related genes using the 10x Genomics Visium platform. K-means clustering of sampling spots corresponds to bundle sheath (BS, dark blue), mesophyll (M, light blue), and water storage (WS, orange) tissues; abundances are shown relative to their observed unique molecule index (UMI) ranges.

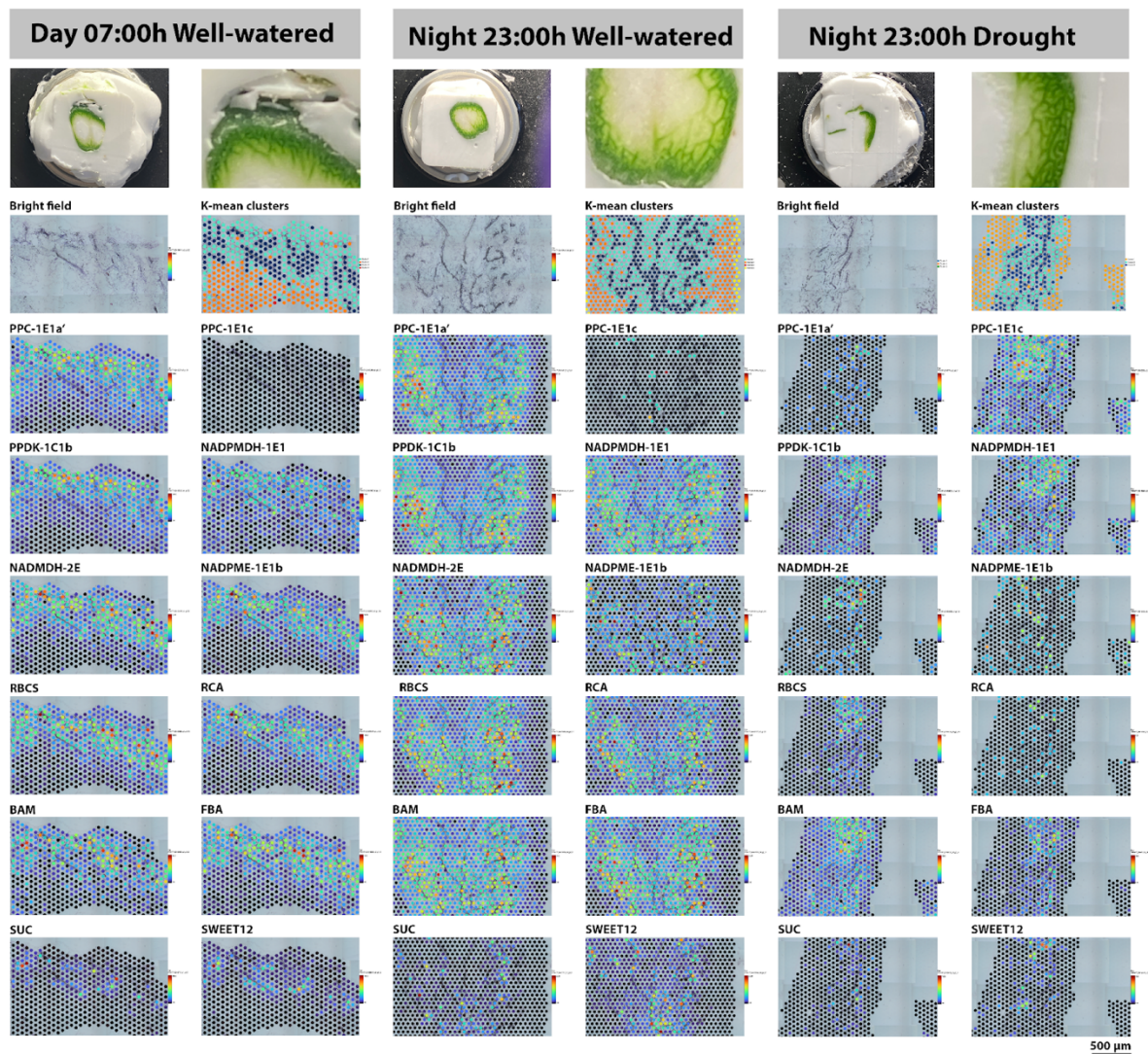
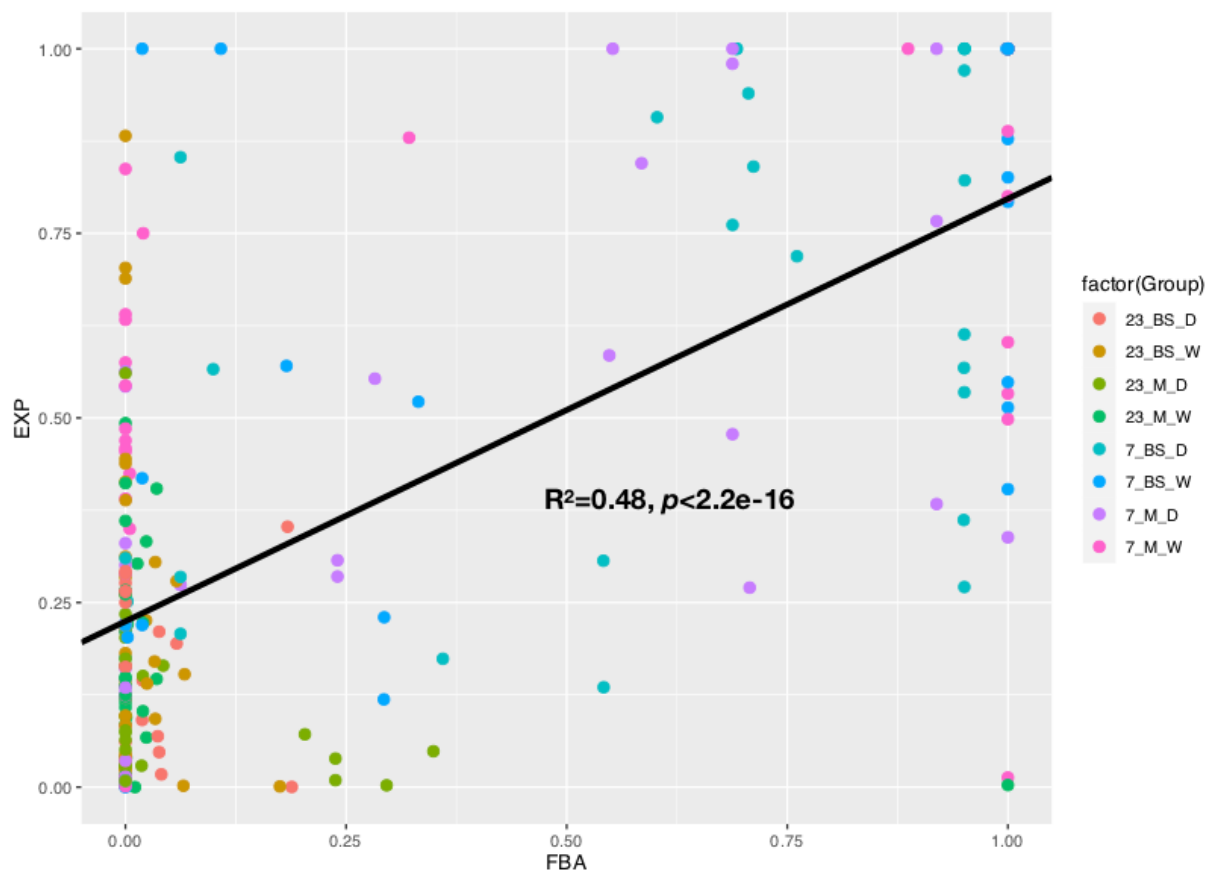


**Fig. S7.**

**Correlations between predicted enzymatic fluxes and estimated gene expression in mesophyll and bundle sheath samples.** Pearson correlation between z-score normalized (mean set to 0, SD set to 1) pFBA results and transcript abundance. The transcript abundances from different orthologs used in the same biochemical reactions were added together to be compared with the pFBA results. 23\_BS\_D: nighttime flux in bundle sheath under drought; 23\_BS\_W: nighttime flux in bundle sheath under well-water; 23\_M\_D: nighttime flux in mesophyll under drought; 23\_M\_W: nighttime flux in mesophyll under well-water; 7\_BS\_D: daytime flux in bundle sheath under drought; 7\_BS\_W: daytime flux in bundle sheath under well-water; 7\_M\_D: daytime flux in mesophyll under drought; 7\_M\_W: daytime flux in mesophyll under well-water;







## Supplementary tables

**Table S1.**

Leaf titratable acidity analysis results. Microequivalents H<sup>+</sup> ( $\mu\text{Eq H}^+$ ) per gram fresh mass was calculated as volume titrant ( $\mu\text{L}$ )  $\times$  titrant molarity (M) / tissue mass (g).

| Sample_id | Treatment | Time (24h) | $\mu\text{Eq H}^+$ |
|-----------|-----------|------------|--------------------|
| POL1-D-7  | drought   | 7h:00      | 76.22              |
| POL1-D-7  | drought   | 7h:00      | 89.52              |
| POL2-D-7  | drought   | 7h:00      | 84.13              |
| POL2-D-7  | drought   | 7h:00      | 71.11              |
| POL1-D-19 | drought   | 19:00:00   | 27.12              |
| POL1-D-19 | drought   | 19:00:00   | 22.26              |
| POL2-D-19 | drought   | 19:00:00   | 41.24              |
| POL2-D-19 | drought   | 19:00:00   | 11.05              |
| POL1-W-7  | watered   | 7h:00      | 24.32              |
| POL1-W-7  | watered   | 7h:00      | 15.63              |
| POL2-W-7  | watered   | 7h:00      | 22.32              |
| POL2-W-7  | watered   | 7h:00      | 16.73              |
| POL1-W-19 | watered   | 19:00:00   | 23.41              |
| POL1-W-19 | watered   | 19:00:00   | 25.96              |
| POL2-W-19 | watered   | 19:00:00   | 16.75              |
| POL2-W-19 | watered   | 19:00:00   | 16.97              |

**Table S2.**

LMD-RNA sequencing and read mapping statistics. BS: bundle-sheath cells, M: mesophyll cells, n<sub>r</sub>: number of reads. T: time; Ind: Plant individual; n<sub>raw</sub>: number of raw reads; n<sub>filtered</sub>: number of reads after filtering; n<sub>aligned</sub>: number of aligned read to the transcriptome; %<sub>al</sub>: percentage of reads aligned to the transcriptome.

| Library_id         | T   | Tissue | Treatment | Ind | n <sub>raw</sub> | n <sub>filtered</sub> | n <sub>aligned</sub> | % <sub>al</sub> |
|--------------------|-----|--------|-----------|-----|------------------|-----------------------|----------------------|-----------------|
| 22-A_PO1-D-7-M     | 7h  | BS     | Drought   | PO1 | 37,306,803       | 32,891,937            | 25,374,659           | 77.10           |
| 5-2-A_PO2-D-7-BS   | 7h  | BS     | Drought   | PO2 | 36,651,612       | 32,289,322            | 23,469,722           | 72.70           |
| 5-A_PO2-D-7-BS     | 7h  | BS     | Drought   | PO2 | 32,587,781       | 28,351,390            | 20,341,689           | 71.70           |
| 10-B_PO2-WW-23-BS  | 7h  | BS     | Watered   | PO1 | 39,734,057       | 23,311,582            | 17,349,512           | 74.40           |
| 12-B_PO1-WW-7-BS   | 7h  | BS     | Watered   | PO1 | 34,351,505       | 23,369,981            | 17,052,138           | 73.00           |
| 4-12-B_PO1-WW-7-BS | 7h  | BS     | Watered   | PO1 | 32,181,954       | 20,082,323            | 14,527,796           | 72.30           |
| 19-B_PO2-WW-7-BS   | 7h  | BS     | Watered   | PO2 | 37,865,848       | 19,888,745            | 14,497,329           | 72.90           |
| 24-A_PO1-D-23-M    | 7h  | M      | Drought   | PO1 | 35,708,771       | 27,081,395            | 22,110,992           | 81.60           |
| 4-2-A_PO2-D-7-M    | 7h  | M      | Drought   | PO2 | 31,310,261       | 27,982,988            | 21,524,928           | 76.90           |
| 6-2-A_PO2-D-7-M    | 7h  | M      | Drought   | PO2 | 35,647,657       | 31,989,325            | 24,098,407           | 75.30           |
| 13-B_PO1-WW-7-M    | 7h  | M      | Watered   | PO1 | 34,519,270       | 22,373,676            | 16,661,642           | 74.50           |
| 15-B_PO1-WW-7-M    | 7h  | M      | Watered   | PO1 | 41,545,559       | 29,425,690            | 21,639,546           | 73.50           |
| 21-A_PO1-D-7-BS    | 7h  | M      | Watered   | PO2 | 39,268,580       | 34,697,032            | 22,238,196           | 64.10           |
| 26-A_PO1-D-23-M    | 23h | BS     | Drought   | PO1 | 38,373,081       | 32,491,941            | 26,358,868           | 81.10           |
| 7-C_PO1-D-23-BS    | 23h | BS     | Drought   | PO1 | 35,134,577       | 15,276,839            | 10,700,178           | 70.00           |
| 15-A_PO2-D-23-BS   | 23h | BS     | Drought   | PO2 | 38,199,397       | 29,299,221            | 21,694,673           | 74.00           |
| 7-A_PO2-D-23-BS    | 23h | BS     | Drought   | PO2 | 35,729,969       | 30,921,888            | 23,884,264           | 77.20           |
| 3-C_PO1-WW-23-BS   | 23h | BS     | Watered   | PO1 | 39,224,405       | 17,905,370            | 13,410,110           | 74.90           |
| 1-12-B_PO1-WW-7-BS | 23h | BS     | Watered   | PO2 | 33,572,474       | 19,664,420            | 14,754,741           | 75.00           |
| 8-B_PO2-WW-23-BS   | 23h | BS     | Watered   | PO2 | 38,190,910       | 20,875,273            | 15,495,580           | 74.20           |
| 25-A_PO1-D-23-BS   | 23h | M      | Drought   | PO1 | 35,543,707       | 31,380,508            | 24,151,852           | 77.00           |
| 2-C_PO1-WW-23-M    | 23h | M      | Drought   | PO1 | 35,114,605       | 12,695,318            | 10,070,151           | 79.30           |
| 8-C_PO1-D-23-M     | 23h | M      | Drought   | PO1 | 48,944,420       | 19,757,250            | 15,312,762           | 77.50           |
| 16-A_PO2-D-23-M    | 23h | M      | Drought   | PO2 | 40,444,993       | 34,196,837            | 27,231,638           | 79.60           |
| 8-A_PO2-D-23-M     | 23h | M      | Drought   | PO2 | 35,841,757       | 30,860,105            | 24,858,317           | 80.60           |
| 20-B_PO2-WW-7-M    | 23h | M      | Watered   | PO1 | 39,592,141       | 22,769,276            | 16,909,912           | 74.30           |
| 11-B_PO2-WW-23-M   | 23h | M      | Watered   | PO2 | 44,046,759       | 28,007,152            | 21,373,120           | 76.30           |
| 9-B_PO2-WW-23-M    | 23h | M      | Watered   | PO2 | 43,071,551       | 24,150,596            | 18,659,731           | 77.30           |



**Table S3.**

Annotation of selected genes with a role or potential role in CCM.

| Phylo-annotation | Uniprot_gene | Description   | unigenes              | Pathway                   |
|------------------|--------------|---|-----------------------|---------------------------|
| ASPAT-3C1        | AATC_DAUCA   | Aspartate aminotransferase, cytoplasmic                                 | TRINITY_DN346_c1_g3   | Carboxylation             |
| BCA-2E3          |              | Beta carbonic anhydrase   | TRINITY_DN889_c1_g2   | Carboxylation             |
| BCA5             | BCA5_ARATH   | Beta carbonic anhydrase 5, chloroplastic                                | TRINITY_DN8226_c0_g1  | Carboxylation             |
| NADPMDH-1E       | MDHP_MESCR   | Malate dehydrogenase [NADP], chloroplastic                              | TRINITY_DN11597_c0_g1 | Carboxylation             |
| PPC-1E1a'        | CAPP_AMAHP   | Phosphoenolpyruvate carboxylase   | TRINITY_DN1747_c2_g1  | Carboxylation             |
| PPC-1E1C         | CAPP2_ARATH  | Phosphoenolpyruvate carboxylase 2                                       | TRINITY_DN3235_c0_g3  | Carboxylation             |
| PPCK-1E          | PPCK1_ARATH  | Phosphoenolpyruvate carboxylase kinase 1                                | TRINITY_DN4567_c3_g1  | Decarboxylation           |
| ASPAT-1E1        |              | Alanine aminotransferase 2, mitochondrial                               | TRINITY_DN18480_c0_g1 | Decarboxylation           |
| DIC-2E           | PUMP5_ARATH  | Mitochondrial uncoupling protein 5                                      | TRINITY_DN1178_c2_g2  | Decarboxylation           |
| NADMDH-1C1       | MDHP_ARATH   | Malate dehydrogenase, chloroplastic                                     | TRINITY_DN2897_c0_g1  | Decarboxylation           |
| NADMDH-2E        |              | Malate dehydrogenase  | TRINITY_DN12466_c1_g1 | Decarboxylation           |
| NADMDH-3C1b      | MDHG_CUCSA   | Malate dehydrogenase, glyoxysomal                                       | TRINITY_DN379_c2_g1   | Decarboxylation           |
| NADMDH-6E1       | MDHC_BETVU   | Malate dehydrogenase, cytoplasmic                                       | TRINITY_DN70366_c1_g1 | Decarboxylation           |
| NADME-2E         | MAON_SOLTU   | NAD-dependent malic enzyme 59 kDa isoform, mitochondrial                | TRINITY_DN17872_c1_g1 | Decarboxylation           |
| NADPME-1E1b      | MAOC_FLAPR   | NADP-dependent malic enzyme, chloroplastic                              | TRINITY_DN1253_c0_g1  | Decarboxylation           |
| NADPME-1E3       | MAOX_VITVI   | NADP-dependent malic enzyme   | TRINITY_DN9969_c0_g1  | Decarboxylation           |
| RBCS-1E          |              | Ribulose biphosphate carboxylase small chain, chloroplastic             | TRINITY_DN6389_c0_g1  | Calvin cycle              |
| RCA-1E           |              | Ribulose biphosphate carboxylase/oxygenase activase, chloroplastic      | TRINITY_DN17967_c2_g1 | Calvin cycle              |
| AK-1E            | KAD2_ARATH   | Adenylate kinase 2, chloroplastic                                       | TRINITY_DN1795_c0_g4  | PEP generation            |
| ALAAAT-1E1       | ALAT2_ARATH  | Alanine aminotransferase 2, mitochondrial                               | TRINITY_DN8707_c0_g1  | PEP generation            |
| BASS-2           | BASS2_ARATH  | Sodium/pyruvate cotransporter BASS2, chloroplastic                      | TRINITY_DN6617_c4_g1  | PEP generation            |
| NHD1-1E1b        | NHD1_ARATH   | Sodium/proton antiporter 1  | TRINITY_DN1372_c2_g1  | PEP generation            |
| PDKRP-1C1        | PDRP1_ORYSI  | Probable pyruvate, phosphate dikinase regulatory protein, chloroplastic | TRINITY_DN7731_c0_g1  | PEP generation            |
| PPDK-1C1b        | PPDK_MESCR   | Pyruvate, phosphate dikinase, chloroplastic                             | TRINITY_DN4872_c3_g1  | PEP generation            |
| PPT-1E2          | PPT2_ORYSJ   | Phosphoenolpyruvate/phosphate translocator 2, chloroplastic             | TRINITY_DN13020_c1_g1 | PEP generation            |
| ERDL             | EDL16_ARATH  | Sugar transporter ERD6-like 16  | TRINITY_DN1122_c0_g1  | Starch/sugar transport    |
| ERDL_pGLC        | ERDL7_ARATH  | Sugar transporter ERD6-like 7   | TRINITY_DN2349_c0_g1  | Starch/sugar transport    |
| GPT-1C1          | GPT2_ARATH   | Glucose-6-phosphate/phosphate translocator 2, chloroplastic             | TRINITY_DN6031_c0_g1  | Starch/sugar transport    |
| GPT-1C2          | GPT2_ARATH   | Glucose-6-phosphate/phosphate translocator 2, chloroplastic             | TRINITY_DN6322_c1_g1  | Starch/sugar transport    |
| MSSP             | MSSP2_ARATH  | Monosaccharide-sensing protein 2  | TRINITY_DN17666_c0_g1 | Starch/sugar transport    |
| TMT              | MSSP2_ARATH  | Monosaccharide-sensing protein 2  | TRINITY_DN6869_c0_g2  | Starch/sugar transport    |
| pGlcT            | PLST4_ARATH  | Plastidic glucose transporter 4   | TRINITY_DN7812_c0_g2  | Starch/sugar transport    |
| SUC              | SUT_SPIOL    | Sucrose transport protein   | TRINITY_DN6710_c1_g1  | Starch/sugar transport    |
| SWEET12          | SWT12_ARATH  | Bidirectional sugar transporter SWEET12                                 | TRINITY_DN19841_c0_g1 | Starch/sugar transport    |
| SWEET13          | SWT13_ARATH  | Bidirectional sugar transporter SWEET13                                 | TRINITY_DN8938_c4_g2  | Starch/sugar transport    |
| TPT-1E2          | TPT_SPIOL    | Triose phosphate/phosphate translocator, chloroplastic                  | TRINITY_DN1249_c1_g1  | Starch/sugar transport    |
| AGPASE           | GLGS2_VICFA  | Glucose-1-phosphate adenyltransferase small subunit 2, chloroplastic    | TRINITY_DN7789_c1_g1  | Starch synthesis          |
| APL              | GLGL1_ARATH  | Glucose-1-phosphate adenyltransferase large subunit 1, chloroplastic    | TRINITY_DN4352_c0_g1  | Starch synthesis          |
| GBSS             | SSG1_MANES   | Granule-bound starch synthase 1, chloroplastic/amyloplastic             | TRINITY_DN11204_c1_g1 | Starch synthesis          |
| ISA              | ISOA1_ARATH  | Isoamylase 1, chloroplastic   | TRINITY_DN4229_c0_g1  | Starch synthesis          |
| SBE              | GLGB1_PEA    | 1,4-alpha-glucan-branching enzyme 1, chloroplastic/amyloplastic         | TRINITY_DN2618_c0_g1  | Starch synthesis          |
| DPE2             | DPE2_ARATH   | 4-alpha-glucanotransferase DPE2   | TRINITY_DN6357_c0_g1  | Transitory starch pathway |
| ENO              | ENO_MESCR    | Enolase   | TRINITY_DN6068_c1_g2  | Transitory starch pathway |
| FBA              | ALFP_ORYSJ   | Fructose-bisphosphate aldolase, chloroplastic                           | TRINITY_DN1271_c0_g1  | Transitory starch pathway |
| HXK              | HXK2_ORYSJ   | Hexokinase-2  | TRINITY_DN7391_c0_g1  | Transitory starch pathway |
| PFK              | PFKA6_ARATH  | ATP-dependent 6-phosphofructokinase 6                                   | TRINITY_DN8265_c0_g1  | Transitory starch pathway |
| PGI              |              | Glucose-6-phosphate isomerase   | TRINITY_DN1518_c1_g1  | Transitory starch pathway |
| PGM              | PGMC_MESCR   | Phosphoglucomutase, cytoplasmic   | TRINITY_DN23625_c0_g1 | Transitory starch pathway |
| TIM              | TPIC_SPIOL   | Triosephosphate isomerase, chloroplastic                                | TRINITY_DN4168_c0_g2  | Transitory starch pathway |
| AMY3             | AMY3_ARATH   | Alpha-amylase 3, chloroplastic  | TRINITY_DN2216_c0_g1  | Starch degradation        |
| BAM              | BAM3_ARATH   | Beta-amylase 3, chloroplastic   | TRINITY_DN1866_c0_g1  | Starch degradation        |
| DSP_SEX4         | DSP4_CASSA   | Phosphoglucan phosphatase DSP4, amyloplastic                            | TRINITY_DN12877_c0_g1 | Starch degradation        |

|            |             |  |                       |                      |
|------------|-------------|--|-----------------------|----------------------|
| LSF        | LSF2_ARATH  | Phosphoglucan phosphatase LSF2, chloroplastic                          | TRINITY_DN2348_c0_g1  | Starch degradation   |
| PHS2       | PHSL2_SOLTU | Alpha-1,4 glucan phosphorylase L-2 isozyme, chloroplastic/amyloplastic | TRINITY_DN12375_c0_g1 | Starch degradation   |
| PWD        | GWD1_CITRE  | Alpha-glucan water dikinase, chloroplastic                             | TRINITY_DN3424_c0_g1  | Starch degradation   |
| ALMT-12E.2 | ALMTC_ARATH | Aluminum-activated malate transporter 12                               | TRINITY_DN10391_c0_g2 | Metabolite transport |
| VHA        |             | V-type proton ATPase subunit   | TRINITY_DN16658_c0_g1 | Metabolite transport |
| AVP1-2E    |             | Pyrophosphate-energized vacuolar membrane proton pump                  | TRINITY_DN1954_c0_g1  | Metabolite transport |
| TDT-1E     | TDT_ARATH   | Tonoplast dicarboxylate transporter                                    | TRINITY_DN161_c0_g1   | Metabolite transport |
| AGT        | SGAT_ARATH  | Serine--glyoxylate aminotransferase                                    | TRINITY_DN6907_c0_g1  | Photorespiration     |
| AGT-1E     | AGT23_ARATH | Alanine--glyoxylate aminotransferase 2 homolog 3, mitochondrial        | TRINITY_DN3579_c0_g1  | Photorespiration     |
| CAT        | CATA2_GOSHI | Catalase isozyme 2   | TRINITY_DN193_c1_g1   | Photorespiration     |
| DIT-1E     | DIT1_SPIOL  | Dicarboxylate transporter 1, chloroplastic                             | TRINITY_DN2503_c0_g1  | Photorespiration     |
| DIT-2E     | DIT2_SPIOL  | Dicarboxylate transporter 2, chloroplastic                             | TRINITY_DN4387_c0_g2  | Photorespiration     |
| GCTV-1E1   | GCST_MESCR  | Aminomethyltransferase, mitochondrial                                  | TRINITY_DN2504_c1_g1  | Photorespiration     |
| GDH-2E     | GCSH_MESCR  | Glycine cleavage system H protein, mitochondrial                       | TRINITY_DN6744_c1_g1  | Photorespiration     |
| GGAT       |             | Glutamate--glyoxylate aminotransferase                                 | TRINITY_DN2102_c0_g1  | Photorespiration     |
| GLDP       | GCSPA_FLAPR | Glycine dehydrogenase (decarboxylating) A, mitochondrial               | TRINITY_DN6006_c0_g1  | Photorespiration     |
| GLN        | GLNA1_LOTJA | Glutamine synthetase cytosolic isozyme                                 | TRINITY_DN4141_c1_g1  | Photorespiration     |
| GOX        | GOX_SPIOL   | Peroxisomal (S)-2-hydroxy-acid oxidase                                 | TRINITY_DN3751_c0_g1  | Photorespiration     |
| GLU        | GLTB_SPIOL  | Ferredoxin-dependent glutamate synthase, chloroplastic                 | TRINITY_DN425_c0_g1   | Photorespiration     |
| GLYK-1E1   | GLYK_ARATH  | D-glycerate 3-kinase, chloroplastic                                    | TRINITY_DN2228_c0_g1  | Photorespiration     |
| HPR-1E     | HPR1_ARATH  | Glycerate dehydrogenase HPR, peroxisomal                               | TRINITY_DN7689_c0_g3  | Photorespiration     |
| LPD-1E     | DLDH1_ARATH | Dihydrolipoyl dehydrogenase 1, mitochondrial                           | TRINITY_DN7076_c1_g1  | Photorespiration     |
| PGLP       | PGP1A_ARATH | Phosphoglycolate phosphatase 1A, chloroplastic                         | TRINITY_DN17754_c0_g1 | Photorespiration     |
| PLGG       |             | Plastidal glycolate/glycerate translocator                             | TRINITY_DN10229_c0_g2 | Photorespiration     |
| SHM-1Eb    | GLYM_SOLTU  | Serine hydroxymethyltransferase, mitochondrial                         | TRINITY_DN302_c1_g2   | Photorespiration     |
| SHM-2E     | GLYC6_ARATH | Serine hydroxymethyltransferase 6                                      | TRINITY_DN1750_c0_g1  | Photorespiration     |
| SHM-3E     |             | Serine hydroxymethyltransferase  | TRINITY_DN3209_c0_g1  | Photorespiration     |
| SHM-4E     | GLYP3_ARATH | Serine hydroxymethyltransferase 3, chloroplastic                       | TRINITY_DN1307_c0_g1  | Photorespiration     |
| ADO        | ADO1_ARATH  | Adagio protein 1   | TRINITY_DN3633_c0_g1  | Light response       |
| BHLH       | BH062_ARATH | Transcription factor bHLH62  | TRINITY_DN360_c1_g1   | Light response       |
| CRY        | CRY1_ARATH  | Cryptochrome-1   | TRINITY_DN2794_c2_g1  | Light response       |
| GATA       |             | Putative GATA transcription factor                                     | TRINITY_DN9003_c0_g1  | Light response       |
| GBF        | GBF1_ARATH  | G-box-binding factor 1   | TRINITY_DN2605_c2_g1  | Light response       |
| GLK        | GLK1_ARATH  | Transcription activator GLK1   | TRINITY_DN969_c0_g1   | Light response       |
| HAT        | HAT1_ARATH  | Homeobox-leucine zipper protein HAT1                                   | TRINITY_DN4311_c1_g1  | Light response       |
| HY         |             | Transcription factor HY5-like  | TRINITY_DN34596_c0_g1 | Light response       |
| MYC        | MYC2_SOLLC  | Transcription factor MYC2  | TRINITY_DN4962_c0_g1  | Light response       |
| NAC        |             | NAC domain-containing protein  | TRINITY_DN3383_c0_g1  | Light response       |
| PHOT       |             | Phototropin-2  | TRINITY_DN282_c3_g1   | Light response       |
| PHY        | PHYA1_TOBAC | Phytochrome A1   | TRINITY_DN2460_c0_g1  | Light response       |
| SIG        | SIGA_ARATH  | RNA polymerase sigma factor sigA                                       | TRINITY_DN4315_c1_g1  | Light response       |
| UVR        | UVR8_ARATH  | Ultraviolet-B receptor UVR8  | TRINITY_DN1267_c1_g1  | Light response       |
| CCA        | LHY_ARATH   | Protein LHY  | TRINITY_DN22210_c0_g1 | Circadian rhythm     |
| CDF        | CDF2_ARATH  | Cyclic dof factor 2  | TRINITY_DN3894_c1_g1  | Circadian rhythm     |
| CK         | CSK21_ARATH | Casein kinase II subunit alpha-1                                       | TRINITY_DN1064_c0_g2  | Circadian rhythm     |
| COL        | COL4_ARATH  | Zinc finger protein CONSTANS-LIKE 4                                    | TRINITY_DN3547_c1_g1  | Circadian rhythm     |
| COP        | COP1_ARATH  | E3 ubiquitin-protein ligase COP1                                       | TRINITY_DN2263_c1_g1  | Circadian rhythm     |
| ELF        |             | Protein EARLY FLOWERING 3  | TRINITY_DN11682_c0_g1 | Circadian rhythm     |
| FT         |             | GlutaminyI-peptide cyclotransferase                                    | TRINITY_DN17372_c0_g1 | Circadian rhythm     |
| GI         | GIGAN_ARATH | Protein GIGANTEA   | TRINITY_DN8078_c0_g1  | Circadian rhythm     |
| LHY        | LHY_ARATH   | Protein LHY  | TRINITY_DN7854_c1_g1  | Circadian rhythm     |
| LUX        | MYBC1_ARATH | Transcription factor MYBC1   | TRINITY_DN1624_c0_g1  | Circadian rhythm     |
| MYB        | MYB4_ARATH  | Transcription repressor MYB4   | TRINITY_DN2554_c0_g1  | Circadian rhythm     |
| RVE        | RVE7L_ARATH | Protein REVEILLE 7-like  | TRINITY_DN10821_c0_g1 | Circadian rhythm     |
| SPA        | SPA1_ARATH  | Protein SUPPRESSOR OF PHYA-105 1                                       | TRINITY_DN1322_c1_g1  | Circadian rhythm     |
| TCP        | PIP25_ARATH | Probable aquaporin PIP2-5  | TRINITY_DN9818_c0_g1  | Circadian rhythm     |

**Table S4.**

Annotation of selected genes differentially expressed across experimental variables without a known role in CCM.

| Uniprot_gene | unigenes              | Description  |
|--------------|-----------------------|--|
| ATHB7        | TRINITY_DN2613_c0_g1  | Homeobox-leucine zipper protein ATHB-7                 |
| BH062        | TRINITY_DN360_c1_g1   | Light response   |
| BHLH         | TRINITY_DN7311_c0_g1  | Light response   |
| CIPK5        | TRINITY_DN1514_c1_g1  | CBL-interacting serine/threonine-protein kinase 5      |
| CIPKB        | TRINITY_DN21721_c0_g1 | CBL-interacting serine/threonine-protein kinase 11     |
| EF1A         | TRINITY_DN8030_c3_g1  | Elongation factor 1-alpha                              |
| EFMT4        | TRINITY_DN2747_c0_g1  | EEF1A lysine methyltransferase 4                       |
| EPS1         | TRINITY_DN2901_c0_g1  | Protein ENHANCED PSEUDOMONAS SUSCEPTIBILITY 1          |
| EXPA2        | TRINITY_DN162_c0_g2   | Expansin-A2  |
| EXTN3        | TRINITY_DN7986_c0_g1  | Extensin-3   |
| HDT1         | TRINITY_DN4285_c1_g2  | Histone deacetylase HDT1                               |
| HSP16        | TRINITY_DN68667_c0_g1 | 18.5 kDa class I heat shock protein                    |
| HYBA1        | TRINITY_DN1856_c0_g1  | Non-reducing end beta-L-arabinofuranosidase            |
| KAI2         | TRINITY_DN7983_c1_g1  | Probable esterase KAI2                                 |
| LSH3         | TRINITY_DN12674_c0_g1 | Protein LIGHT-DEPENDENT SHORT HYPOCOTYLS 3             |
| LSH6         | TRINITY_DN12674_c0_g1 | Protein LIGHT-DEPENDENT SHORT HYPOCOTYLS 6             |
| MYB4         | TRINITY_DN2554_c0_g1  | Transcription repressor MYB4                           |
| NAP2         | TRINITY_DN7132_c0_g5  | NAC domain-containing protein 2                        |
| NCED1        | TRINITY_DN2687_c0_g2  | 9-cis-epoxycarotenoid dioxygenase NCED1, chloroplastic |
| NFD4         | TRINITY_DN13340_c0_g1 | Protein NUCLEAR FUSION DEFECTIVE 4                     |
| NIA          | TRINITY_DN6723_c1_g1  | Nitrate reductase [NADH]                               |
| NLTP         | TRINITY_DN79002_c1_g1 | Probable non-specific lipid-transfer protein AKCS9     |
| PAR1         | TRINITY_DN1658_c0_g1  | Phenylacetaldehyde reductase                           |
| PER2         | TRINITY_DN11931_c0_g1 | Cationic peroxidase 2                                  |
| PGLR         | TRINITY_DN2996_c0_g1  | Probable polygalacturonase                             |
| PUMP4        | TRINITY_DN12670_c1_g1 | Mitochondrial uncoupling protein 4                     |
| PURA2        | TRINITY_DN2249_c0_g2  | Adenylosuccinate synthetase 2, chloroplastic           |
| RL261        | TRINITY_DN8213_c0_g1  | 60S ribosomal protein L26-1                            |
| RL9          | TRINITY_DN56917_c0_g1 | 60S ribosomal protein L9                               |
| RS3A         | TRINITY_DN11338_c0_g2 | 40S ribosomal protein S3a                              |
| SCL15        | TRINITY_DN19737_c0_g1 | Scarecrow-like protein 15                              |
| VPE1         | TRINITY_DN9527_c0_g1  | Vacuolar-processing enzyme                             |
| WRKY7        | TRINITY_DN13587_c0_g1 | Probable WRKY transcription factor 7                   |
| WTR32        | TRINITY_DN5341_c0_g2  | WAT1-related protein At4g08300                         |

**Table S5.**

Sequencing and reads mapping statistics across Visium mRNA libraries.

| Sample ID        | n_spots | m_Genes | n_reads   | m_reads_per_spot | n_reads_map_confidently | Fraction Reads in Spots Under Tissue | Total Genes Detected | Median UMI Counts per Spot | Fraction of Spots Under Tissue |
|------------------|---------|---------|-----------|------------------|-------------------------|--------------------------------------|----------------------|----------------------------|--------------------------------|
| S1_A1_PO1_7h_WW  | 1426    | 53      | 150099218 | 105258.92        | 0.04                    | 0.92                                 | 138                  | 368.5                      | 0.29                           |
| S2_B1_PO1_23h_WW | 1972    | 57      | 199760709 | 101298.53        | 0.03                    | 0.98                                 | 139                  | 352.5                      | 0.40                           |
| S3_D1_PO1_23h_D  | 1751    | 26      | 121129683 | 69177.43         | 0.01                    | 0.80                                 | 136                  | 44                         | 0.35                           |
| S4_A1_PO1_7h_WW  | 1925    | 40      | 192674632 | 100090.72        | 0.03                    | 0.90                                 | 137                  | 167                        | 0.39                           |
| S5_B1_PO1_23h_WW | 3757    | 34      | 322216248 | 85764.24         | 0.02                    | 0.96                                 | 139                  | 95                         | 0.75                           |
| S6_D1_PO1_23h_D  | 1575    | 25      | 117371115 | 74521.34         | 0.01                    | 0.75                                 | 135                  | 41                         | 0.32                           |

**Table S6**

Sensitivity analysis FBA results of major reactions for different drought conditions. Well-watered: well-watered conditions. Drought20%: 20% stomata closure compared to well-watered condition; Drought45%: 45% stomata closure compared to well-watered condition, which is the regular drought condition; Drought70%: 70% stomata closure compared to well-watered condition. Unit for the fluxes is mmol gDW<sup>-1</sup>day<sup>-1</sup>. Major reactions are Phloem output, PEP carboxylation, Rubisco carboxylation and CO<sub>2</sub> absorption directly from the atmosphere (CO<sub>2</sub>). All the scenarios are modelled in mesophyll (M) or bundle sheath (BS) at daytime (day) and night time (night)

| SCENARIO                       | Well-watered | Drought20% | Drought45% | Drought70% |
|--------------------------------|--------------|------------|------------|------------|
| Phloem output                  | 3.42         | 3.29       | 3.14       | 2.99       |
| PEP carboxylation_M_day        | 127.67       | 100.00     | 70.00      | 40.00      |
| PEP carboxylation_BS_day       | 0            | 0          | 0          | 0          |
| PEP carboxylation_M_night      | 0            | 20.27      | 47.23      | 74.12      |
| PEP carboxylation_BS_night     | 8.55         | 8.86       | 8.68       | 8.58       |
| Rubisco carboxylation_M_day    | 0            | 0          | 0          | 0          |
| Rubisco carboxylation_BS_day   | 140.53       | 136.94     | 133.51     | 130.07     |
| Rubisco carboxylation_M_night  | 0            | 0          | 0          | 0          |
| Rubisco carboxylation_BS_night | 0            | 0          | 0          | 0          |
| CO <sub>2</sub> _M_day         | 127.67       | 100.00     | 70.00      | 40.00      |
| CO <sub>2</sub> _BS_day        | 0            | 0          | 0          | 0          |
| CO <sub>2</sub> _M_night       | -7.18        | 16.07      | 40.79      | 65.51      |
| CO <sub>2</sub> _BS_night      | 0            | 0          | 0          | 0          |

**Table S7.**

FBA results for major reactions of additional modelling scenarios in mesophyll (M) or bundle sheath (BS) at daytime (day) and night time (night). Major reactions are Phloem output, PEP carboxylation (PEP), Rubisco carboxylation (Rubisco) and CO<sub>2</sub> absorption directly from the atmosphere (CO<sub>2</sub>). All the scenarios are modelling under the drought condition (45% stomata closure). Scenario 1): blocking malate transfer between mesophyll and bundle sheath (bMalT). Scenario 2): blocking malate storage in mesophyll (bMS), bundle sheath (bBSS), or both (bMBSS). Scenario 3): CAM with C<sub>3</sub> or C<sub>4</sub> anatomy. C3+CAM: both C<sub>3</sub> and CAM activity (both daytime and night time CO<sub>2</sub> uptake) allowed with a C<sub>3</sub> anatomy (CO<sub>2</sub> directly diffuses into mesophyll, bundle sheath is considered an inner mesophyll with a longer distance to stomata); CAM\_C3: only CAM (nighttime CO<sub>2</sub> uptake) occurs with C<sub>3</sub> anatomy ; CAM\_C4: CAM process (nighttime CO<sub>2</sub> uptake) with C<sub>4</sub> anatomy (CO<sub>2</sub> can not directly diffuse into bundle sheath); C4+CAM\_C4: C4 and CAM (both daytime and night time CO<sub>2</sub> uptake) can occur with C<sub>4</sub> anatomy (CO<sub>2</sub> can not directly diffuse into bundle sheath), which can be used as the reference for all the above scenarios.

| SCENARIO                | bMalT  | bMS    | bBSS   | bMBSS  | C3+CAM_ | C3    | CAM_C3 | CAM_C4 | C4+CAM_ | C4 |
|-------------------------|--------|--------|--------|--------|---------|-------|--------|--------|---------|----|
| <b>Phloem output</b>    | 3.14   | 3.14   | 3.14   | 1.64   | 2.56    | 2.48  | 2.79   | 3.14   |         |    |
| <b>PEP_M_day</b>        | 70.00  | 70.00  | 70.00  | 70.00  | 0       | 0     | 0      | 70.00  |         |    |
| <b>PEP_BS_day</b>       | 0      | 0      | 0      | 0      | 0       | 0     | 0      | 0      |         |    |
| <b>PEP_M_night</b>      | 47.49  | 49.53  | 50.72  | 0      | 29.91   | 77.05 | 108.65 | 47.23  |         |    |
| <b>PEP_BS_night</b>     | 8.42   | 6.38   | 5.19   | 2.79   | 4.28    | 29.99 | 9.76   | 8.68   |         |    |
| <b>Rubsico_M_day</b>    | 0      | 0      | 0      | 0      | 88.94   | 85.33 | 0      | 0      |         |    |
| <b>Rubsico_BS_day</b>   | 133.51 | 133.51 | 133.51 | 74.4   | 36.40   | 33.49 | 125.49 | 133.51 |         |    |
| <b>Rubsico_M_night</b>  | 0      | 0      | 0      | 0      | 0       | 0     | 0      | 0      |         |    |
| <b>Rubsico_BS_night</b> | 0      | 0      | 0      | 0      | 0       | 0     | 0      | 0      |         |    |
| <b>CO2_M_day</b>        | 70.00  | 70.00  | 70.00  | 70.00  | 40.00   | 0     | 0      | 70.00  |         |    |
| <b>CO2_BS_day</b>       | 0      | 0      | 0      | 0      | 30.00   | 0     | 0      | 0      |         |    |
| <b>CO2_M_night</b>      | 40.79  | 40.79  | 40.79  | -12.22 | 24.83   | 67.89 | 98.48  | 40.79  |         |    |
| <b>CO2_BS_night</b>     | 0      | 0      | 0      | 0      | -4.42   | 19.77 | 0      | 0      |         |    |

**Table S8.**

Sensitivity analysis of FBA results of major reactions for Rubisco carboxylation to oxygenation ratio ( $V_o/V_c$ ) for  $C_4$  in bundle sheath. Major reactions are Phloem output, PEP carboxylation, Rubisco carboxylation and  $CO_2$  absorption directly from the atmosphere ( $CO_2$ ). All the scenarios are modelling under the drought condition in mesophyll (M) or bundle sheath (BS) at daytime (day) and night time (night). Unit for the fluxes is  $mmol\ gDW^{-1}day^{-1}$ .

| $V_o/V_c$                             | 10     | 20     | 40     | 80     | 200    |
|---------------------------------------|--------|--------|--------|--------|--------|
| <b>Phloem output</b>                  | 3.14   | 3.32   | 3.43   | 3.48   | 3.51   |
| <b>PEP carboxylation_M_day</b>        | 70.00  | 70.00  | 70.00  | 70.00  | 70.00  |
| <b>PEP carboxylation_BS_day</b>       | 0      | 0      | 0      | 0      | 0      |
| <b>PEP carboxylation_M_night</b>      | 47.23  | 54.48  | 58.23  | 60.15  | 61.31  |
| <b>PEP carboxylation_BS_night</b>     | 8.68   | 8.64   | 8.66   | 8.67   | 8.67   |
| <b>Rubisco carboxylation_M_day</b>    | 0      | 0      | 0      | 0      | 0      |
| <b>Rubisco carboxylation_BS_day</b>   | 133.51 | 137.53 | 136.63 | 140.71 | 141.36 |
| <b>Rubisco carboxylation_M_night</b>  | 0      | 0      | 0      | 0      | 0      |
| <b>Rubisco carboxylation_BS_night</b> | 0      | 0      | 0      | 0      | 0      |
| <b>CO2_M_day</b>                      | 70.00  | 70.00  | 70.00  | 70.00  | 70.00  |
| <b>CO2_BS_day</b>                     | 0      | 0      | 0      | 0      | 0      |
| <b>CO2_M_night</b>                    | 40.79  | 47.44  | 50.91  | 52.69  | 53.77  |
| <b>CO2_BS_night</b>                   | 0      | 0      | 0      | 0      | 0      |

## Online Supplementary Materials

Available on Dryad (<https://datadryad.org>) DOI: 10.5061/dryad.931zcrjm6

### ONLINE TABLES:

#### Captions for Online Table S1:

Estimated counts of reads mapped to each unigene per LMD library.

#### Captions for Online Table S2:

Transcriptome-wide gene annotation and differential expression statistics.

#### Captions for Online Table S3:

CCM-related (or hypothetically related) genes. Functional and phylogenetic annotation into gene lineage and/or gene families. Differential expression statistics.

#### Captions for Online Table S4:

Representative contigs (highest expressed) by gene lineage and/or gene family. Differential expression statistics.

#### Captions for Online Table S5:

FBA results summary.

### ONLINE VISIUM METADATA:

Space Ranger Output files. Metadata containing quantification and analysis summaries of transcripts abundance across Visium samples. Files can be visualized using the software Loupe Browser (10X Genomics; <https://www.10xgenomics.com/products/loupe-browser>). The list of gene features to display in Loupe are found in table S3

#### Captions for Online Data S1

Visium spatial gene expression: Loupe file with metadata for 7h well-watered sample replicate 1

#### Captions for Online Data S2

Visium spatial gene expression: Loupe file with metadata for 7h well-watered sample replicate 2

#### Captions for Online Data S3

Visium spatial gene expression: Loupe file with metadata for 23h well-watered sample replicate 1

#### Captions for Online Data S4

Visium spatial gene expression: Loupe file with metadata for 23h well-watered sample replicate 2

#### Captions for Online Data S5

Visium spatial gene expression: Loupe file with metadata for 23h droughted sample replicate 1



**Captions for Online Data S6**

Visium spatial gene expression: Loupe file with metadata for 23h droughted sample replicate 2